Research in Astron. Astrophys. **2012** Vol. **12** No. **12**, 1625–1636
http://www.raa-journal.org *http://www.iop.org/journals/raa*

***R**esearch in*
***A**stronomy and*
***A**strophysics*

Hydrodynamical wind in magnetized accretion flows with convection

Shahram Abbassi[1,2] and Amin Mosallanezhad[1,3]

[1] School of Physics, Damghan University, P.O. Box 36715-364, Damghan, Iran
[2] School of Astronomy, Institute for Research in Fundamental Sciences, P.O. Box 19395-5531, Tehran, Iran; *abbassi@ipm.ir*
[3] Center for Excellence in Astronomy & Astrophysics (CEAA - RIAAM), P.O. Box 55134-441, Maragha, Iran

Received 2012 May 1; accepted 2012 May 30

Abstract The existence of outflow and magnetic fields in the inner region of hot accretion flows has been confirmed by observations and numerical magnetohydrodynamic (MHD) simulations. We present self-similar solutions for radiatively inefficient accretion flows (RIAFs) around black holes in the presence of outflow and a global magnetic field. The influence of outflow is taken into account by adopting a radius that depends on mass accretion rate $\dot{M} = \dot{M}_0(r/r_0)^s$ with $s > 0$. We also consider convection through a mixing length formula to calculate convection parameter $\alpha_{\rm con}$. Moreover we consider the additional magnetic field parameters $\beta_{r,\varphi,z}\big[= c^2_{r,\varphi,z}/(2c^2_{\rm s})\big]$, where $c^2_{r,\varphi,z}$ are the Alfvén sound speeds in three directions of cylindrical coordinates. Our numerical results show that by increasing all components of the magnetic field, the surface density and rotational velocity increase, but the sound speed and radial infall velocity of the disk decrease. We have also found that the existence of wind will lead to reduction of surface density as well as rotational velocity. Moreover, the radial velocity, sound speed, advection parameter and the vertical thickness of the disk will increase when outflow becomes important in the RIAF.

Key words: accretion: accretion flow — wind: outflow — convection: MHD

1 INTRODUCTION

Observations of accreting black holes with different masses show impressive similarities of data which point to an identical physical process in the accretion flow. Also, black hole accretion disks exhibit a great variety of physical conditions, so we may have a variety of accretion regimes. Existing theories describe different regimes of black hole accretion flows, which can be realized under different physical conditions. Accreting black holes in nearby galactic nuclei and low-state X-ray binaries are much dimmer than the standard Shakura-Sunyaev disk model would predict. A phenomenon of under-luminous accreting black holes in X-ray binaries and super-massive black holes in galactic nuclei has stimulated the recent investigations of radiatively inefficient accretion flows (RIAFs) (see Narayan et al. 1998; Kato et al. 2008 for reviews). In such a flow, radiative losses are small because of the low particle density in the accretion flow at low accretion rates. Contrary to the standard Shakura-Sunyaev disk model, which successfully explains sources that emit soft radiation and which

are luminous in X-rays, models of RIAFs are used to explain a significant deficit of radiation observed in some X-ray sources. A particular example of such underluminous sources is the Galactic center, Sagittarius A^*, which hosts a 2×10^6 solar mass black hole. The Galactic center has a luminosity that is well below the estimated value based on the Shakura-Sunyaev accretion disk model (Melia & Falcke 2001).

Advection-dominated accretion flows (ADAFs) are in the opposite regime compared to that of the standard model. In the standard model, the flow is described in such a way that the heat generated by the viscosity radiates out of the system immediately after its generation (Shakura & Sunyaev 1973). These ADAFs occur in two regimes depending on their mass accretion and optical depth. Actually, the optical depths of accretion flows are highly dependent on their accretion rates. In a situation with a high mass-accretion rate, the optical depth becomes very high and the radiation generated by the accretion flow can be trapped within the disk. In this case, the optical depth is very large, and photons, which carry most of the internal energy, are trapped inside the inflowing matter and cannot be radiated away. This type of model is called a 'slim disk,' or optically thick ADAF. Although the radiative efficiency of an optically thick ADAF is also low, we usually only call the optically thin ADAF an RIAF. In the limit of low mass-accretion rate, the disk becomes optically thin. In this case, the cooling time of accretion flows is longer than the accreting timescale. The energy generated by accretion flows therefore remains mostly in the disks, and the disks cannot radiate their energy efficiently. This type of accretion flow is named an RIAF. This type of accretion flow has been investigated by many authors (Narayan & Yi 1994; Abramowicz et al. 1995; Chen 1995). At the same time as the ADAF model was proposed, it was realized that the ADAFs are likely to be convectively unstable in the radial direction because of the inward increase of the entropy of accreting gas (Igumenshchev & Abramowicz 1999; Stone et al. 1999; Igumenshchev et al. 2003). Most recent work focusing on the convective instability was performed by Yuan & Bu (2010). Two and three dimensional simulations of a low-viscosity RIAF confirmed the convective instability in these flows (Igumenshchev et al. 1996; Igumenshchev & Abramowicz 2000; McKinney & Gammie 2002). Narayan et al. (2000) and Quataert & Gruzinov (2000) constructed another analytical model of RIAFs which was based on a self-similar solution called the convection dominated accretion flow (CDAF). CDAFs consist of a hot plasma at about virial temperature and have a flattened time-averaged radial density profile, $\rho \propto r^{-1/2}$, where ρ is the density and r is the radius. In CDAFs, most of the energy which is released in the innermost region of the accretion flow is then transported outward by convective motion.

The self-similar CDAF model, being the same as other self-similar models, is very clear and instructive, but it has some limitations. It is only a local, not a global solution for an RIAF, in the sense that it can only be valid for a region far from boundaries. Hence, it cannot reproduce the physical behavior of an accretion flow, which is transonic radial motion — the most fundamental feature of a black hole accretion flow. Abramowicz et al. (1995) did suggest a two-zone structure for an RIAF: an outer convection dominated zone and an inner advection dominated zone separated at a transition radius $\sim 50 r_g$.

There is also evidence that the process of mass accretion via a disk is often and perhaps always associated with mass loss from the disk in the form of a wind or a jet. Mass loss appears to be a common phenomenon among astrophysical accretion disk systems. These mass-loss mechanisms are observed in microquasars, young stellar objects and even from brown dwarfs (Ferrari 1998; Bally et al. 2007; Whelan et al. 2005). It has long been obvious that a disk wind/outflow contributes to loss of mass, angular momentum, and thermal energy from accretion disks (e.g. Piran 1978; ; Foschini 2011; Knigge 1999). Various driving sources have been proposed, including thermal, radiative and magnetic ones. Traditionally the name of the wind depends on its driving force. In this paper we will follow the hydrodynamical (thermal) wind which has been discussed by many authors (e.g. Meier 1979, 1982; Fukue 1989; Takahara et al. 1989). There are some observational implications of outflows in accreting systems. The accretion rates onto neutron stars in soft X-ray

transients in quiescent states seem to be smaller than those of white dwarfs in cataclysmic variables with comparable orbital periods, since the typical luminosities in both cases are similar, in spite of their difference of gravitational potential by three orders of magnitude (Loeb et al. 2001). This indicates significant outflows in accretion flows, where $s \sim 1$. Outflows from hot accretion flows also seem to be common in the nuclei of galaxies. The compact radio/infrared/X-ray source Sgr A*, harboring a super-massive black hole in the center of our Galaxy, also has moderate mass loss. Its mass accretion rate at $r \leq 10$ AU ($\sim 100\ r_{\rm s}$, where $r_{\rm s}$ is the Schwarzschild radius) is estimated as $\dot{M} \sim 10^{-7} M_{\odot}\ {\rm yr}^{-1}$ by a Faraday rotation measurement (Marrone et al. 2006). On the other hand, the Bondi accretion rate expected by the hot ambient gas around $r \sim 0.04$ pc ($\sim 10^5\ r_{\rm s}$) is $\dot{M} \sim 10^{-5} M_{\odot}\ {\rm yr}^{-1}$ (Baganoff et al. 2003). This significant difference between the inner and outer mass accretion rates indicates mass loss from the accretion flow due to the outflow (Kawabata & Mineshige 2009). As a result of mass loss, the accretion rate, $\dot{M}$, is no longer constant in radius r. It is often expressed as $\dot{M} \propto r^s$ with s being a constant of the order of unity (Blandford & Begelman 1999).

Early work on disk accretion to a black hole argued that a large-scale magnetic field originating from the interstellar medium, or even the central engine, would be dragged inward and greatly compressed near the black hole by the accreting plasma (Bisnovatyi-Kogan & Ruzmaikin 1974, 1976). So large-scale B-fields have an important role in the dynamics and structure of a hot accretion flow since the flow is highly ionized. The effect of magnetic fields on the structure of ADAFs was also studied (Balbus & Hawley 1998; Shadmehri 2004; Meier 2005; Shadmehri & Khajenabi 2005, 2006; Ghanbari et al. 2007; Abbassi et al. 2008, 2010; Xie & Yuan 2008; Bu et al. 2009).

In this paper we will discuss the properties of CDAFs in a general large-scale magnetic field with hydrodynamical wind. We will concentrate on the self-similar solution. This study is motivated by recent works of Zhang & Dai (2008) who showed there is an effect of large scale magnetic fields on the CDAFs that can be modeled with a constructive self-similar solution. Because CDAFs are usually modeled for outer regions of RIAFs where the hydrodynamical outflow becomes important, we investigate the role of outflow in the dynamical structure of magnetized CDAFs. We will show the basic equations and self-similar solutions in Sections 2 and 3 respectively, and conclusions are given in Section 4.

2 BASIC EQUATIONS

We are interested in analyzing the structure of a magnetized hot accretion flow bathed in a global magnetic field where convection and wind play an important role in transport of energy and angular momentum. Suppose there is a rotating and accreting disk around a compact Schwarzchild black hole of mass M_*. Thus, for a steady axisymmetric accretion flow, i.e., $\partial/\partial t = \partial/\partial\varphi = 0$, we can write the standard equations in the cylindrical coordinates (r, φ, z) centered on the accreting object. We vertically integrate the flow equations so all the physical variables become only functions of the radial distance r. Moreover, we consider a magnetic field in the disk with three components, B_r, B_φ and B_z. We also neglect relativistic effects and Newtonian gravity is considered adequate in the radial direction.

Under these assumptions, the equation of continuity will be

$$\frac{\partial}{\partial r}(r\Sigma v_r) + \frac{1}{2\pi}\frac{\partial \dot{M}_w}{\partial r} = 0\,, \tag{1}$$

where Σ is the surface density at the cylindrical radius r, which is defined as $\Sigma = 2\rho H$, ρ is the midplane density, H is the disk half-thickness and v_r is the radial infall velocity. Also the mass loss rate by outflow/wind is represented by $\dot{M}_w$, so

$$\dot{M}_w(r) = \int 4\pi r' \dot{m}_w(r') dr'\,, \tag{2}$$

where $\dot{m}_w(r)$ is the mass loss rate per unit area from each disk surface. We can write the dependence of accretion rate as follows (Blandford & Begelman 1999; Shadmehri 2008)

$$\dot{M} = -2\pi r \Sigma v_r = \dot{M}_0 \left(\frac{r}{r_0}\right)^s , \tag{3}$$

where $\dot{M}_0$ is the mass accretion rate at the outer radius of the disk r_0 and s is a constant of order unity (Blandford & Begelman 1999). For a disk without outflow/wind, $s = 0$ and in the presence of the outflow/wind, $s > 0$ (e.g. Fukue 2004). The observed broadband spectra of Sgr A* and soft X-ray transients can also be fitted by RIAF models with moderate outflows, $s \sim 0.3 - 0.4$, if the direct heating of electrons in an RIAF is efficient (Quataert & Narayan 1999; Yuan et al. 2003; Kawabata & Mineshige 2009).

Considering Equations (1)–(3), we can write

$$\dot{m}_w = s \frac{\dot{M}_0}{4\pi r_0^2} \left(\frac{r}{r_0}\right)^{s-2} . \tag{4}$$

The equation of motion in the radial direction is

$$v_r \frac{dv_r}{dr} = \frac{v_\varphi^2}{r} - \frac{GM_*}{r^2} - \frac{1}{\Sigma}\frac{d}{dr}(\Sigma c_s^2) - \frac{1}{2\Sigma}\frac{d}{dr}(\Sigma c_\varphi^2 + \Sigma c_z^2) - \frac{c_\varphi^2}{r} , \tag{5}$$

where v_φ is the rotational velocity, $c_{\rm s}$ is the sound speed, which is defined as $c_{\rm s}^2 \equiv p_{\rm gas}/\rho$, with $p_{\rm gas}$ being the gas pressure. Here, c_r, c_φ and c_z are Alfvén sound speeds in three directions of cylindrical coordinates and are defined as

$$c_{r,\varphi,z}^2 = \frac{B_{r,\varphi,z}^2}{4\pi\rho} = \frac{2p_{{\rm mag}_{r,\varphi,z}}}{\rho} , \tag{6}$$

where $p_{{\rm mag}_{r,\varphi,z}}$ are the magnetic pressure in three directions. Considering outflow/wind and convection, the angular transfer equation can be written as

$$\Sigma v_r \frac{d}{dr}(r v_\varphi) = -\frac{1}{r}\frac{d}{dr}(J_{\rm vis}) - \frac{1}{r}\frac{d}{dr}(J_{\rm con}) + r\sqrt{\Sigma} c_r \frac{d}{dr}(\sqrt{\Sigma} c_\varphi) + \Sigma c_r c_\varphi - \frac{l^2(r\Omega)}{2\pi}\frac{d\dot{M}_w}{dr} , \tag{7}$$

where $J_{\rm vis}$ and $J_{\rm con}$ are viscous and convective angular momentum fluxes, respectively, which are defined as

$$J_{\rm vis} = -\nu \Sigma r^3 \frac{d\Omega}{dr} \tag{8}$$

and

$$J_{\rm con} = -\nu_{\rm con} \Sigma r^{3(1+g)/2} \frac{d}{dr}(\Omega r^{3(1-g)/2}) . \tag{9}$$

Here, ν is the kinematic viscosity coefficient, $\nu = \alpha c_s H$, with α being the constant Shakura & Sunyaev parameter, $\nu_{\rm con}$ is the convective diffusion coefficient, and g is the index that describes the convective angular momentum transport. When $g = 1$, the flux of angular momentum due to convection is

$$J_{\rm con} = -\nu_{\rm con} \Sigma r^3 \frac{d\Omega}{dr} . \tag{10}$$

The above equation implies that the convective angular momentum flux is oriented down the angular velocity gradient. For a quasi-Keplerian angular velocity, where $\Omega \propto r^{-3/2}$, angular momentum is transported outward. When $g = -1/3$, the convective angular momentum flux can be written as

$$J_{\rm con} = -\nu_{\rm con} \Sigma r \frac{d(r^2\Omega)}{dr} . \tag{11}$$

This equation represents that the convective angular momentum flux is oriented down the specific angular momentum gradient. For a quasi-Keplerian angular velocity, $\Omega \propto r^{3/2}$, angular momentum is transported inward. Convection generally transports angular momentum inward (or outward) for $g < 0$ (or > 0), and the specific case $g = 0$ corresponds to zero angular momentum transport (Narayan et al. 2000).

The last term on the right side of the angular transfer equation, Equation (7), also represents angular momentum carried by the outflowing material. Here $l = 0$ corresponds to a non-rotating wind and $l = 1$ to outflowing material that carries away the specific angular momentum (see e.g., Knigge 1999).

By integrating the hydrostatic balance over z, we have

$$\Omega_K^2 H^2 - \frac{1}{\sqrt{\Sigma}} c_r \frac{d}{dr}\left(\sqrt{\Sigma} c_z\right) H - \left[c_{\rm s}^2 + \frac{1}{2}\left(c_r^2 + c_\varphi^2\right)\right] = 0\,. \tag{12}$$

By considering outward energy due to convection and energy loss by outflows, the energy equation becomes

$$\Sigma v_r T \frac{dS}{dr} + \frac{1}{r}\frac{d}{dr}(r F_{\rm con}) = f(\nu + g\nu_{\rm con})\Sigma r^2 \left(\frac{d\Omega}{dr}\right)^2 - \frac{1}{2}\eta \dot{m}_w(r) v_K^2(r)\,. \tag{13}$$

In the above equation T is temperature, S is the specific entropy and $F_{\rm con}$ is the convective energy flux which is defined as

$$F_{\rm con} = -\nu_{\rm con}\Sigma T \frac{dS}{dr}\,, \tag{14}$$

where

$$T\frac{dS}{dr} = \frac{1}{\gamma - 1}\frac{dc_{\rm s}^2}{dr} - \frac{c_{\rm s}^2}{\rho}\frac{d\rho}{dr}\,. \tag{15}$$

Here γ is the ratio of specific heats. As was mentioned, the last term on the right hand side of the energy equation is the energy loss due to wind or outflow (Knigge 1999). Depending on the energy loss mechanism, dimensionless parameter η may change. In our case, we consider it as a free parameter (Knigge 1999). Also in the energy equation, we still neglect the Joule heating rate.

We adopt the assumptions of Narayan et al. (2000) and Lu et al. (2004) for the convective diffusion coefficient, $\nu_{\rm con}$, which is defined as

$$\nu_{\rm con} = \frac{L_{\rm M}^2}{4}(-N_{\rm eff}^2)^{1/2}\,. \tag{16}$$

Here $N_{\rm eff}$ is the effective frequency of convective blobs and $L_{\rm M}$ is the characteristic mixing length. The effective frequency of convective blobs will be

$$N_{\rm eff}^2 = N^2 + \kappa^2\,, \tag{17}$$

with N and κ being the Brunt-Väisälä frequency and epicyclic frequency respectively, which are defined as

$$N^2 = -\frac{1}{\rho}\frac{dp_g}{dr}\frac{d}{dr}\ln\left(\frac{p_g^{1/\gamma}}{\rho}\right)\,, \tag{18}$$

$$\kappa^2 = 2\Omega^2 \frac{d\ln(r^2\Omega)}{d\ln r}\,. \tag{19}$$

For a non-Keplerian flow $\kappa \neq \Omega$, but for a quasi-Keplerian case ($\Omega \propto r^{-3/2}$), $\kappa = \Omega$ (Narayan et al. 2000; Lu et al. 2004). Note that convection in flows appears with $N_{\rm eff}^2 < 0$.

In addition, the characteristic mixing length $L_{\rm M}$ in terms of the pressure scale height, $H_{\rm p}$, can be written as

$$L_{\rm M} = 2^{-1/4} l_{\rm M} H_{\rm p} \tag{20}$$

and

$$H_{\rm p} = -\frac{dr}{d\ln p_g}\,, \tag{21}$$

where $l_{\rm M}$ is the dimensionless mixing length parameter and its value is estimated to be equal to $\sqrt{2}$ in ADAFs (Narayan et al. 2000; Lu et al. 2004). The convective diffusion coefficient can also be written in a form similar to the usual viscosity of Shakura & Sunyaev (1973),

$$\nu_{\rm con} = \alpha_{\rm con} c_{\rm s} H\,, \tag{22}$$

where $\alpha_{\rm con}$ is a dimensionless coefficient that describes the strength of convective diffusion. The $\alpha_{\rm con}$ coefficient can be obtained by Equations (16) and (22)

$$\alpha_{\rm con} = \frac{L_{\rm M}^2}{4c_{\rm s}H}(-N_{\rm eff}^2)^{1/2}\,. \tag{23}$$

Finally we can write the three components of the induction equation, $(\dot{B}_r, \dot{B}_\varphi, \dot{B}_z)$, to measure the rate of escape for the magnetic field,

$$\dot{B}_r = 0\,, \tag{24}$$

$$\dot{B}_\varphi = \frac{d}{dr}(v_\varphi B_r - v_r B_\varphi)\,, \tag{25}$$

$$\dot{B}_z = -\frac{d}{dr}(v_r B_z) - \frac{v_r B_z}{r}\,. \tag{26}$$

Here $\dot{B}_{r,\varphi,z}$ is the rate of escaping/creation of the field due to magnetic instability or a dynamo effect. Now we have a set of magnetohydrodynamic (MHD) equations that describe the structure of magnetized CDAFs. The solutions to these equations are strongly correlated to viscosity, convection, magnetic field strength $\beta_{r,\varphi,z}$ and the degree of advection f. We seek a self-similar solution for the above equations. In the next section we will present self-similar solutions to these equations.

3 SELF-SIMILAR SOLUTIONS

3.1 Analysis

In order to have a better understanding of the physical processes taking place in our disks, we seek self-similar solutions of the above equations. The self-similar method has a wide range of applications for the full set of MHD equations although it is unable to describe the global behavior of accretion flows since no boundary conditions have been taken into account. However, as long as we are not interested in the behavior of the flow near the boundaries, these solutions are still valid.

We assume that the physical quantities can be expressed as a power law of radial distance, i.e., r^ν, where ν is determined by substituting the similarity solutions into the main equations and solving the resulting algebraic equations. Therefore, we can write the similarity solutions as

$$\Sigma(r) = c_0 \Sigma_0 \left(\frac{r}{r_0}\right)^{s-\frac{1}{2}}\,, \tag{27}$$

$$v_r(r) = -c_1 \sqrt{\frac{GM_*}{r_0}} \left(\frac{r}{r_0}\right)^{-\frac{1}{2}}\,, \tag{28}$$

$$v_\varphi(r) = c_2\sqrt{\frac{GM_*}{r_0}}\left(\frac{r}{r_0}\right)^{-\frac{1}{2}}, \tag{29}$$

$$c_s^2(r) = c_3^2\left(\frac{GM_*}{r_0}\right)\left(\frac{r}{r_0}\right)^{-1}, \tag{30}$$

$$c_{r,\varphi,z}^2(r) = \frac{B_{r,\varphi,z}^2}{4\pi\rho} = 2\beta_{r,\varphi,z}c_3^2\left(\frac{GM_*}{r_0}\right)\left(\frac{r}{r_0}\right)^{-1}, \tag{31}$$

$$H(r) = c_4 r_0\left(\frac{r}{r_0}\right), \tag{32}$$

where constants c_0, c_1, c_2, c_3 and c_4 will be determined later from the main MHD equation. Σ_0 and r_0 are exploited to write the equations in non-dimensional forms and the constants $\beta_{r,\varphi,z}$ measure the ratio of the magnetic pressure in three directions to the gas pressure, i.e., $\beta_{r,\varphi,z} = p_{\mathrm{mag}_{r,\varphi,z}}/p_{\mathrm{gas}}$.

In addition, the rate of field escaping/creation $\dot{B}_{r,\varphi,z}$ is assumed to have a form

$$\dot{B}_{r,\varphi,z} = \dot{B}_{r0,\varphi0,z0}\left(\frac{r}{r_0}\right)^{\frac{1}{2}(s-\frac{11}{2})}, \tag{33}$$

where $\dot{B}_{r0,\varphi0,z0}$ is a constant.

By substituting the above self-similar solutions in the continuity, momentum, angular momentum, hydrostatic balance and energy equations of the disk, we obtain the following system of dimensionless equations to be solved for c_0, c_1,c_2 c_3 and c_4:

$$c_0c_1 = \dot{m}, \tag{34}$$

$$-\frac{1}{2}c_1^2 = c_2^2 - 1 - \left[\left(s-\frac{3}{2}\right) + \left(s-\frac{3}{2}\right)\beta_z + \left(s+\frac{1}{2}\right)\beta_\varphi\right]c_3^2, \tag{35}$$

$$\left(sl^2 - \frac{1}{2}\right)\frac{\dot{m}}{c_0}c_2 = -\frac{3}{2}\left(s+\frac{1}{2}\right)(\alpha + g\alpha_{\mathrm{con}})c_2c_3c_4 + \left(s+\frac{1}{2}\right)c_3^2(\beta_r\beta_\varphi)^{1/2}, \tag{36}$$

$$c_4 = \frac{1}{2}c_3\left\{\left[\left(s-\frac{3}{2}\right)^2\beta_r\beta_z c_3^2 + 4(1+\beta_r+\beta_\varphi)\right]^{1/2} + c_3\left(s-\frac{3}{2}\right)(\beta_r\beta_z)^{1/2}\right\}, \tag{37}$$

$$\left(\frac{1}{\gamma-1} + s - \frac{3}{2}\right)\left\{(s-1)\alpha_{\mathrm{con}}c_3^3c_4 + c_1c_3^2\right\} = \frac{9}{4}fc_2^2c_3c_4(\alpha + g\alpha_{\mathrm{con}}) - \frac{1}{4}s\eta\frac{\dot{m}}{c_0}, \tag{38}$$

where $\dot{m}$ is the non-dimensional mass accretion rate, which is defined as

$$\dot{m} = \frac{\dot{M}_0}{2\pi r_0\Sigma_0\sqrt{GM_*/r_0}}. \tag{39}$$

If we solve the self-similar structure of the magnetic field escape rate, we will have

$$\dot{B}_{0r} = 0, \tag{40}$$

$$\dot{B}_{0\varphi} = \frac{1}{2}\left(s-\frac{7}{2}\right)\frac{GM_*}{r_0^{5/2}}c_3\sqrt{\frac{4\pi c_0\Sigma_0}{c_4}}\left(c_2\sqrt{\beta_r} + c_1\sqrt{\beta_\varphi}\right), \tag{41}$$

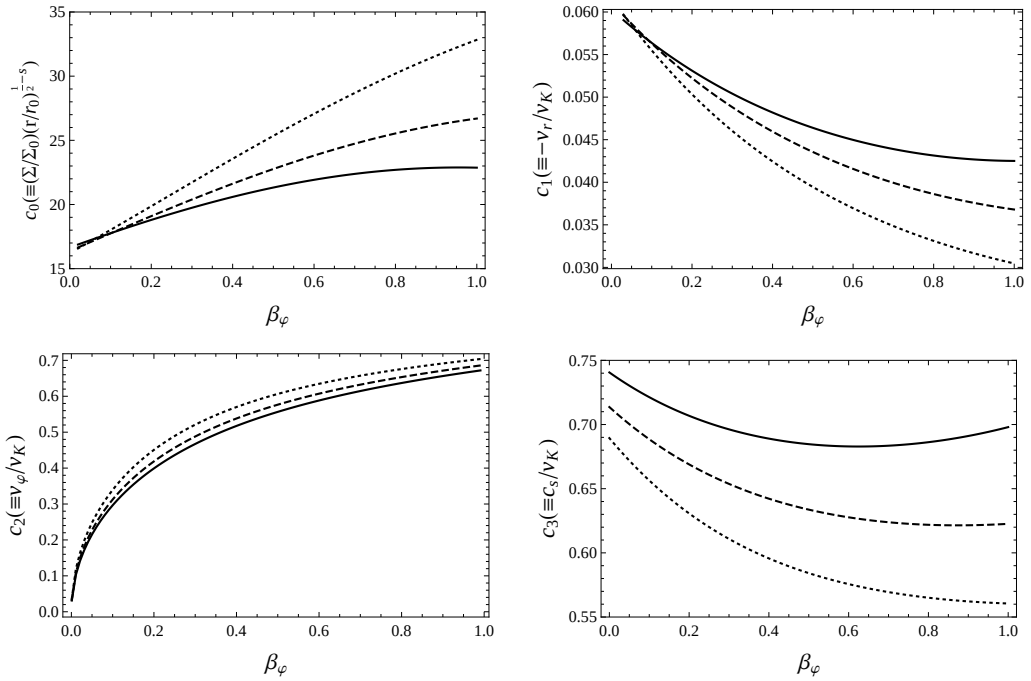

Fig. 1 Numerical coefficients c_i as a function of magnetic parameter β_φ for several values of s. The dotted, dashed and solid lines correspond to $s = 0.0, 0.1$ and 0.2, respectively. Parameters are set as $\alpha = 0.5$, $\gamma = 1$, $g = -1/3$, $\beta_r = \beta_z = 0.4$, $\eta = l = 1$ and $f = 1$.

$$\dot{B}_{0z} = \frac{1}{2}\left(s - \frac{3}{2}\right) c_1 c_3 \frac{GM_*}{r_0^{5/2}} \sqrt{\frac{4\pi\beta_z c_0 \Sigma_0}{c_4}}\,. \tag{42}$$

We can solve these simple equations numerically so that the physical solutions can be clearly interpreted. Without mass outflow and magnetic field, i.e. $s = l = \eta = \beta_r = \beta_\varphi = \beta_z = 0$, the equations and their similarity solutions are reduced to the Narayan et al. solution (Narayan et al. 2000). Also in the absence of outflow they are reduced to the case of Zhang & Dai (2008).

Now we can analyze the behavior of the solutions in the presence of wind, convection and a global magnetic field. The parameters of our model are the standard viscosity parameter α, the advection parameter f, the ratio of the specific heats γ, the mass-loss parameter s, the degree that magnetic pressure contributes to the gas pressure in three dimensions using cylindrical coordinates, β_r, β_φ and β_z and l, η parameters correspond to the cases of wind and outflow.

3.2 Numerical Results

In Figure 1 the physical variables of surface density (c_0), radial infall velocity (c_1), rotational velocity (c_2) and sound speed (c_3) are shown as a function of toroidal magnetic field parameter β_φ for several values of wind parameter s, i.e., $s = 0$ (dotted line, no wind), $s = 0.1$ (dashed line) and $s = 0.2$ (solid line). Four panels of Figure 1 are set as $\alpha = 0.5$, $\gamma = 1$, $\beta_r = \beta_z = 0.4$, $\eta = l = 1$ and $f = 1$. By adding the toroidal magnetic field parameter β_φ, we see that the surface density and rotational velocity of the disk increase, although the radial infall velocity and sound speed both decrease.

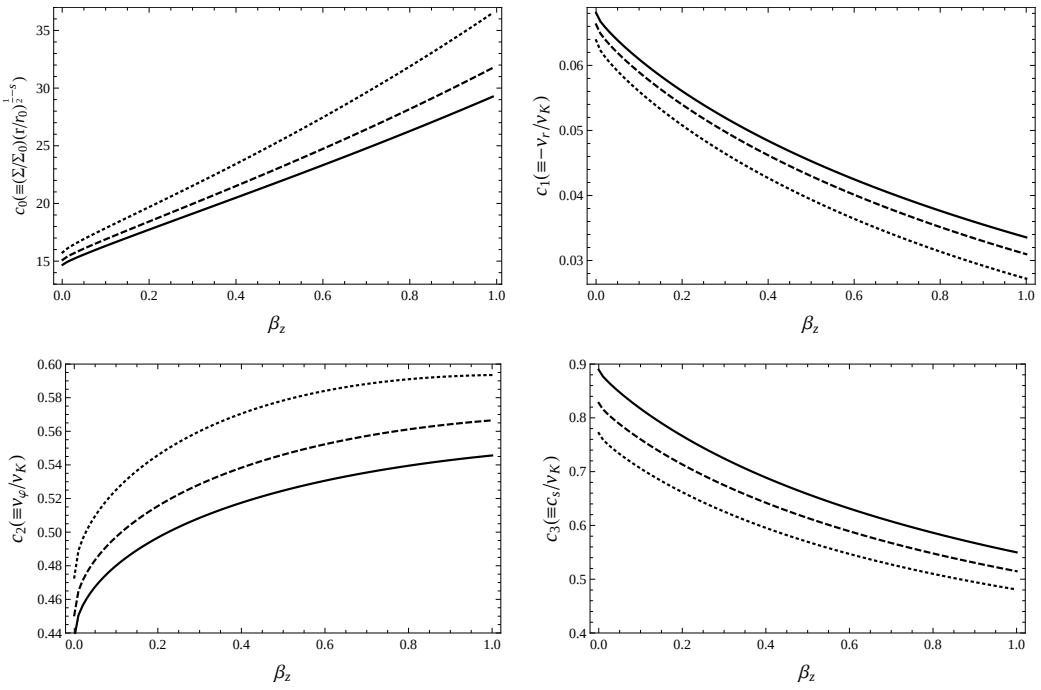

Fig. 2 Numerical coefficients c_i as a function of magnetic parameter β_z for several values of s. The dotted, dashed and solid lines correspond to $s = 0.0, 0.1$ and 0.2, respectively. Parameters are set as $\alpha = 0.5, \gamma = 1, g = -1/3, \beta_r = \beta_\varphi = 0.4, \eta = l = 1$ and $f = 1$.

On the other hand, the radial flow decreases when the toroidal magnetic field becomes large. This is because the magnetic tension term dominates the magnetic pressure term in the radial momentum equation. We can see that by adding the influences of the magnetic field (adding β_φ), the rotation velocity will increase. This is because the disk should rotate faster than the case without the magnetic field which results in magnetic tension.

In Figure 1 we also studied the effect of parameter $s = 0$ on physical coefficients. As was mentioned, the value of s measures the strength of wind/outflow and a larger s denotes a stronger wind. We can see that for stronger outflow ($s = 0$) , the reduction of surface density is more evident. We see that the convective model of accretion flows with the presence of wind leads to slower rotation than the case without wind, and adding wind leads to enhanced accretion velocity. The sound speed of the disk also increases for stronger outflows.

The physical variables as a function of magnetic field parameter β_z and several values of mass loss parameter are shown in Figure 2. As can be seen, a strong z-component of magnetic field leads to an increase in both surface density and rotational velocity, but the radial infall velocity of materials and sound speed of the disk decrease.

Figure 3 shows how the coefficients c_i depend on the magnetic field parameter in the radial direction β_r for several values of outflow parameter s. We see that the surface density and rotational velocity rise when the magnetic field parameter β_r increases, while the sound speed and accretion velocity will decrease. According to Figures 1, 2 and 3, by adding all the components of the magnetic field, the surface density and rotational velocity increase but the sound speed and radial infall velocity of the disk will decrease.

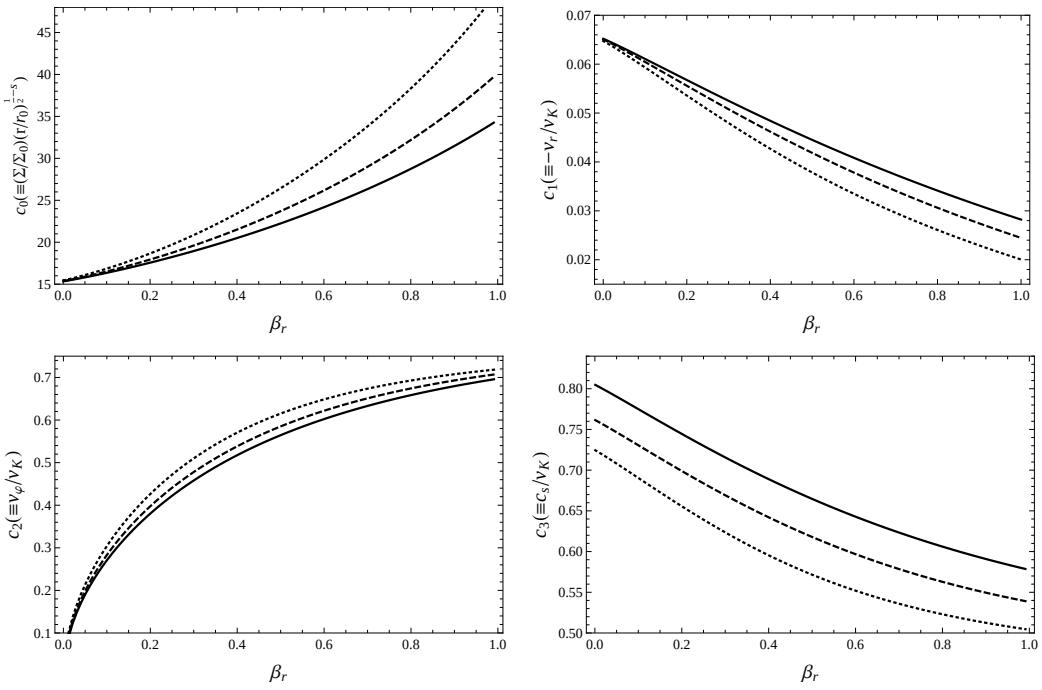

Fig. 3 Numerical coefficients c_i as a function of magnetic parameter β_r for several values of s. The dotted, dashed and solid lines correspond to $s = 0.0, 0.1$ and 0.2, respectively. Parameters are set as $\alpha = 0.5$, $\gamma = 1$, $g = -1/3$, $\beta_\varphi = \beta_z = 0.4$, $\eta = l = 1$ and $f = 1$.

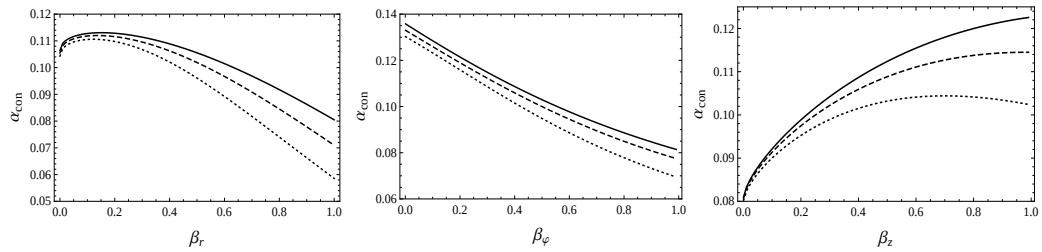

Fig. 4 The convective coefficient $\alpha_{\rm con}$ as a function of magnetic parameters β_r, β_φ and β_z for several values of wind parameter s. The dotted, dashed and solid lines correspond to $s = 0.0, 0.1$ and 0.2 respectively. Parameters are set as $\alpha = 0.5$, $\gamma = 1$, $g = -1/3$, $\eta = l = 1$ and $f = 1$.

In Figure 4, we have plotted the convective parameter $\alpha_{\rm con}$ versus magnetic field parameters β_r, β_φ and β_z for several values of s. As can be seen, when the magnetic field parameter β_r becomes stronger, the convective parameter decreases (left panel). By adding the toroidal component of the magnetic field β_φ, the convective parameter $\alpha_{\rm con}$ also decreases (middle panel), although by adding the z-component of the magnetic field, $\alpha_{\rm con}$ increases (right panel).

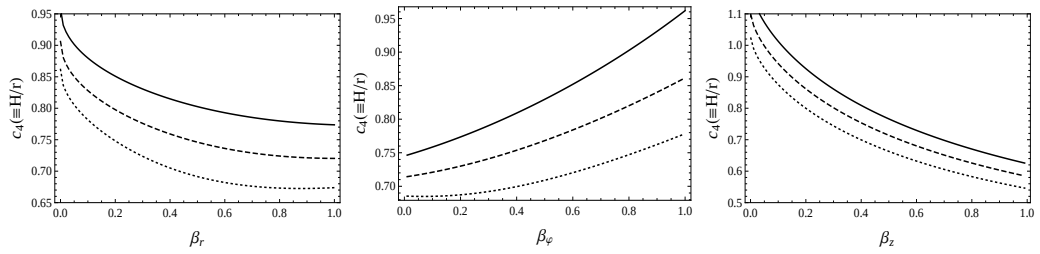

Fig. 5 The behavior of H/r as a function of magnetic parameters β_r, β_φ and β_z for several values of wind parameter s. The dotted, dashed and solid lines correspond to $s = 0.0, 0.1$ and 0.2 respectively. Parameters are set as $\alpha = 0.5$, $\gamma = 1$, $g = -1/3$, $\eta = l = 1$ and $f = 1$.

Figure 5 shows that the disk thickness is enhanced with the toroidal magnetic field parameter β_φ and wind parameter s (middle panel). Also, the radial and vertical components of the magnetic field decrease the vertical thickness of the accretion disk (left and right panels).

4 CONCLUSIONS

The CDAF model consistently represents RIAFs into black holes in the framework of viscous flow. We have considered the radial structure of RIAFs based on a self-similar analysis. Some approximations were made in order to simplify the main equations. We assumed an axially symmetric, static disk with the α-prescription of viscosity, $\nu = \alpha c_{\rm s} H$. A set of similarity solutions was presented for such a configuration. We have extended self similar solutions of Akizuki & Fukue (2006); Zhang & Dai (2008) and Faghei & Omidvand (2012) to model the dynamical structure of the CDAFs. We ignored the relativistic effects and the self-gravity of the disks.

We have found that by increasing all components of magnetic field, the surface density and rotational velocity increase, although the sound speed and radial infall velocity of the disk decrease. We have also shown that the existence of wind will lead to reduction of surface density as well as rotational velocity. Moreover the radial velocity, sound speed, advection parameter and vertical thickness of the disk will increase when outflow becomes important in the RIAF.

In this manuscript, we have examined the effect of large-scale B-fields on the convective structure with wind and outflow. In the future it would be interesting to study how these effects would change the observational appearance of the flow.

Although we have made some simplifying assumptions in order to treat the problem analytically, our self-similar solution shows large-scale magnetic fields can really change typical behavior of the physical quantities of a hot accretion flow. Not only the surface density of the disk changes, but also the rotational and the radial velocities significantly change because of the magnetic fields, which means that any realistic model for a hot disk should consider the possible effects of the magnetic fields.

References

Abbassi, S., Ghanbari, J., & Najjar, S. 2008, MNRAS, 388, 663
Abbassi, S., Ghanbari, J., & Ghasemnezhad, M. 2010, MNRAS, 409, 1113
Abramowicz, M. A., Chen, X., Kato, S., Lasota, J.-P., & Regev, O. 1995, ApJ, 438, L37
Akizuki, C., & Fukue, J. 2006, PASJ, 58, 469
Baganoff, F. K., Maeda, Y., Morris, M., et al. 2003, ApJ, 591, 891

Balbus S. A., & Hawley, J. F. 1998, RMP, 70, 1
Bally, J., Reipurth, B., & Davis, C. J. 2007, Protostars and Planets V (University Arizona Press), 215
Bisnovatyi-Kogan, G. S., & Ruzmaikin, A. A. 1974, Ap&SS, 28, 31
Bisnovatyi-Kogan, G. S., & Ruzmaikin, A. A. 1976, Ap&SS, 42, 401
Blandford, R. D., & Begelman, M. C. 1999, MNRAS, 303, L1
Bu, D.-F., Yuan, F., & Xie, F.-G. 2009, MNRAS, 392, 325
Chen, X. 1995, MNRAS, 275, 641
Faghei, K., & Omidvand, M. 2012, Ap&SS, 341, 363 (arXiv:1204.0743)
Ferrari, A. 1998, ARA&A, 36, 539
Foschini, L. 2011, RAA (Research in Astronomy and Astrophysics), 11, 1266
Fukue, J. 1989, PASJ, 41, 123
Fukue, J. 2004, PASJ, 56, 181
Ghanbari, J., Salehi, F., & Abbassi, S. 2007, MNRAS, 381, 159
Igumenshchev, I. V., & Abramowicz, M. A. 1999, MNRAS, 303, 309
Igumenshchev, I. V., & Abramowicz, M. A. 2000, ApJS, 130, 463
Igumenshchev, I. V., Chen, X., & Abramowicz, M. A. 1996, MNRAS, 278, 236
Igumenshchev, I. V., Narayan, R., & Abramowicz, M. A. 2003, ApJ, 592, 1042
Kato, S., Fukue, J., & Mineshige, S. 2008, Black-Hole Accretion Disks — Towards a New Paradigm (Kyoto Univ. Press)
Kawabata, R., & Mineshige, S. 2009, PASJ, 61, 1135
Knigge, C. 1999, MNRAS, 309, 409
Loeb, A., Narayan, R., & Raymond, J. C. 2001, ApJ, 547, L151
Lu, J.-F., Li, S.-L., & Gu, W.-M. 2004, MNRAS, 352, 147
Marrone, D. P., Moran, J. M., Zhao, J.-H., & Rao, R. 2006, ApJ, 640, 308
McKinney, J. C., & Gammie, C. F. 2002, ApJ, 573, 728
Meier, D. L. 1979, ApJ, 233, 664
Meier, D. L. 1982, ApJ, 256, 706
Meier, D. L. 2005, Ap&SS, 300, 55
Melia, F., & Falcke, H. 2001, ARA&A, 39, 309
Narayan, R., Igumenshchev, I. V., & Abramowicz, M. A. 2000, ApJ, 539, 798
Narayan, R., Mahadevan, R., & Quataert, E. 1998, in Theory of Black Hole Accretion Disks, eds. M. A. Abramowicz, G. Bjornsson, & J. E. Pringle (Cambridge Univ. Press), 148
Narayan, R., & Yi, I. 1994, ApJ, 428, L13
Piran, T. 1978, ApJ, 221, 652
Quataert, E., & Gruzinov, A. 2000, ApJ, 539, 809
Quataert, E., & Narayan, R. 1999, ApJ, 520, 298
Shadmehri, M. 2004, A&A, 424, 379
Shadmehri, M. 2008, Ap&SS, 317, 201
Shadmehri, M., & Khajenabi, F. 2005, MNRAS, 361, 719
Shadmehri, M., & Khajenabi, F. 2006, ApJ, 637, 439
Shakura, N. I., & Sunyaev, R. A. 1973, A&A, 24, 337
Stone, J. M., Pringle, J. E., & Begelman, M. C. 1999, MNRAS, 310, 1002
Takahara, F., Rosner, R., & Kusunose, M. 1989, ApJ, 346, 122
Whelan, E. T., Ray, T. P., Bacciotti, F., et al. 2005, Nature, 435, 652
Xie, F.-G., & Yuan, F. 2008, ApJ, 681, 499
Yuan, F., & Bu, D.-F. 2010, MNRAS, 408, 1051
Yuan, F., Quataert, E., & Narayan, R. 2003, ApJ, 598, 301
Zhang, D., & Dai, Z. G. 2008, MNRAS, 388, 1409